Click-chemistry with an active site variant of azurin

Jongh, T.E. de; Roon, A. van; Prudêncio, M.; Ubbink, M.; Canters, G.W.

DOI: 10.1002/ejic.200600574

Click Chemistry with an Active Site Variant of Azurin

Thyra E. de Jongh,[a] Anne-Marie M. van Roon,[a][‡] Miguel Prudêncio,[a][‡‡] Marcellus Ubbink,[a] and Gerard W. Canters*[a]

Keywords: Metalloproteins / Protein structures / Zinc / Copper / Metal replacement

The active site of the blue copper protein azurin (Azu) from *Pseudomonas aeruginosa* consists of a Cu ion immobilized by bonds to four amino acid side chains. The protein assists in electron transfer *in vivo*. Replacement of Cu-ligand His117 by a Gly makes the Cu site accessible for exogenous ligands. Incubation of the H117G Azu with *n*-alkane linkers carrying imidazole groups at opposite ends leads to the formation of noncovalently linked Azu dimers. The active site of H117G Azu is vulnerable to Cu-catalyzed oxidative attack. Replacement of Cu^{II} by Zn^{II} leads to stable dimers, whose structures have been determined by X-ray diffraction. These structures are reported here. The similarity in the structure of the active site between the wild type (*wt*) Zn-Azu and the dimer is remarkable in light of the different relation of the coordinating imidazole to the protein framework (covalently attached vs. exogenous origin, respectively). The part of the "ligand loop" running from amino acid 116 to 121 has acquired increased flexibility in the mutant. The connected subunits have adopted an unexpected orientation relative to each other.

Introduction

When applied to proteins, "click" chemistry can provide decisively new insight in structure and function. Click chemistry refers to the technique by which a side chain or a prosthetic group is removed from a protein framework, either chemically or by site-directed mutagenesis, and the resulting gap is filled by exogenous compounds. In this way, modified flavins or heme groups have been inserted into the apo forms of flavoproteins and heme proteins.[1–3] It allows the modification of active sites of enzymes in a simple and straightforward manner. When the prosthetic group is extended with a linker ("hot wire"), click chemistry can also allow for the connection of the active site of an enzyme to a partner molecule or to an electrode.

In copper-containing proteins, the active site consists of one or more Cu ions that are immobilized in the protein through coordinate bonds to side chains. By replacing one of these side chains by a small amino acid (Gly or Ala), the Cu centre becomes directly accessible for exogenous ligands. The technique has been successfully applied to the active site of blue copper proteins and to the type-1 site of the Cu-containing nitrite reductase.[4,5]

[a] Leiden Institute of Chemistry, Leiden University, Gorlaeus Laboratories
Einsteinweg 55, P. O. Box 9502, 2300 RA Leiden, The Netherlands
Fax: +31-71-527-4349
E-mail: canters@chem.leidenuniv.nl
[‡] Current address: MRC Laboratory of Molecular Biology, Hills Road, Cambridge CB2 2QH, United Kingdom
[‡‡]Current address: Unidade de Malária, Instituto de Medicina Molecular, Faculdade de Medicina de Lisboa, Av. Prof. Egas Moniz, 1649-028 Lisbon, Portugal

In the case of the small blue copper protein azurin (Azu) from *Pseudomonas aeruginosa*, His117 has been subjected to such modification. In Azu the Cu is bound by the Sγ and Sδ atoms of Cys112 and Met121, respectively, and the Nδ atoms of the residues His46 and His117. There is also a weak interaction with the backbone carbonyl of Gly45.[6] Azu is an electron-transfer protein, possibly involved in oxidative stress response.[7] With many electron-transfer proteins, a small part of the prosthetic group (flavin in the case of flavodoxins or heme in the case of cytochromes, for instance) or the active centre (the Fe-S cluster in ferredoxins or the Cu site in cupredoxins, for instance) is directly accessible from the outside. In Azu this part of the structure is formed by the Cu-ligand His117. It protrudes through the protein surface at a shallow depression in the so-called hydrophobic patch. His117 provides for electronic coupling with the Cu and, presumably, represents the site where physiological partners dock.[8,9]

Replacement of His117 by a Gly results in a slightly destabilized form of the protein with a Cu site that has been classified as Type-2 with spectral characteristics (EPR, UV/Vis) that clearly differ from the native protein but revert to those of the native protein upon incubation with imidazole.[4,10,11] So far, attempts to determine the structure of this Azu variant by crystallography failed because the destabilized Cu site appears vulnerable to Cu^{2+} catalyzed oxidative attack by oxygen, which converts the Cys112 sulfur into a sulfonate.[12] NMR studies showed an increased mobility of the ligand loop (running from Cys112 to Met121) on which His117 is located.[13] Click chemistry can enable the formation of protein multimers by using multifunc-

tional linkers. It has, for instance, been shown that the incubation of H117G Azu with 1,ω-di(imidazol-1-yl)-*n*-alkane linkers leads to formation of dimers when butane, pentane and hexane are employed as the alkane moiety.[14]

In principle, the Cu-catalyzed oxidative modification of the Cu site in H117G Azu should be avoidable by substituting the Cu by the redox-inactive Zn. It is known that in the small blue copper proteins this substitution leads to minimal distortion of the native structure and of the active site in particular, the changes in the latter being limited to a shortening of the M^{2+}–Gly45 carbonyl bond and an elongation of the M^{2+}–Sδ(Met121) bond.[15]

Here we report on the preparation and characterization of the 1,5-di(imidazol-1-yl)pentane (1,5-dip) and 1,6-di(imidazol-1-yl)hexane (1,6-dih) linked dimers of Zn-H117G Azu. The results provide insight into the structural and dynamic properties of the H117G Azu variant. In particular, they give an unexpected perspective on the mobility of the ligand loop in native and H117G Azu.

Results

Dimerization of Zn-H117G Azurin

As Zn-H117G Azu is colourless, coordination of the imidazole-based linkers can not be followed by the green-to-blue optical transition that occurs upon coordination of

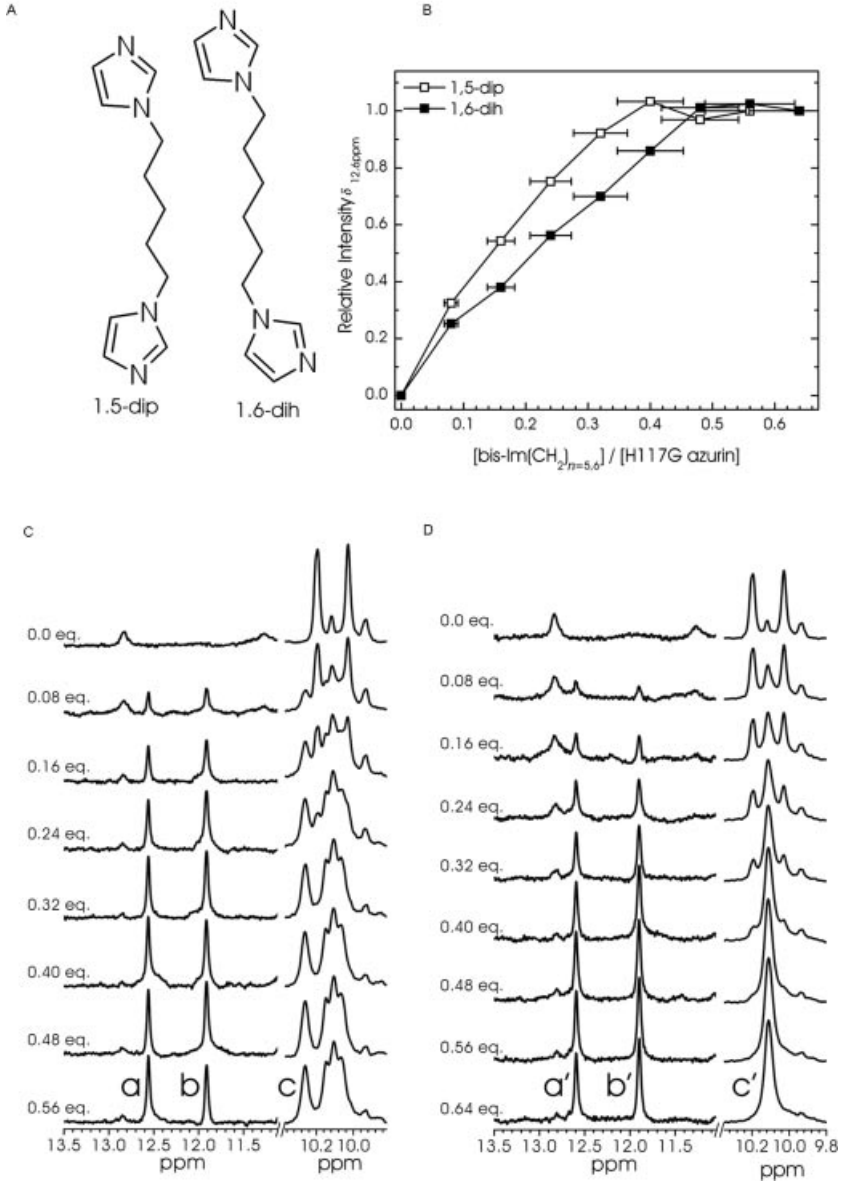

Figure 1. Titration of Zn-H117G Azu with linkers 1,5-dip and 1,6-dih (A): (B) Relative averaged intensity of resonance a [1,5-dip (□)] and resonance a′ [1,6-dih (■)] of Zn-H117G at increasing ratios of linker to protein (see also panels C and D). (C) and (D): High-field regions of the ^{1}H NMR spectra of 1 mM Zn-H117G Azu upon titration with 1,5-dip (C) or 1,6-dih (D), at pH 6.5 and 305 K for different molar equivalents of linker to Zn-H117G Azu.

imidazole to Cu^{II}-H117G Azurin.[4,10] Instead, ligand binding was monitored by ^1H NMR spectroscopy. Addition of 0.7 molar equiv. of 1,5-dip or 1,6-dih to apo-H117G Azu had no discernible effect on the ^1H NMR spectrum (not shown), whereas subsequent addition of a slight molar excess of $Zn(SO_4)_2$ to the sample led to the occurrence of several new protein resonances in the downfield region of the spectrum (Figure 1C, D). This demonstrates the formation of a new species for which Zn is required. The new species exhibits a 3–4 Hz increase in line width corresponding to a 40–60% increase in T_2^{-1}. As the latter varies proportionally with the rotational correlation time, τ_c, the increase in line width reflects an increase in τ_c. While doubling of the molecular weight should be accompanied with a doubling of τ_c for a spherical molecule, the smaller increase may reflect the nonspherical shape of the dimer. The line broadening and the appearance of new resonances confirm the formation of Zn^{II}-His117Gly Azu dimers noncovalently linked by di(imidazolyl)alkanes.

To check the stoichiometry, samples of Zn-H117G Azu were titrated with 1,5-dip and 1,6-dih. The NMR spectra are shown in Figure 1C and Figure 1D. In the course of the 1,5-dip titration, the signals at 12.56, 11.91 and 10.26 ppm (Figure 1C: signals a, b and c) grew, while the peaks around 10.1 ppm, consisting of a number of partially overlapping signals, changed shape. Similar observations were made for signals at 12.59, 11.90 and 10.11 ppm (Figure 1D: signals a′, b′ and c′) in the case of the 1,6-dih titration. In the latter case, signal c′ almost completely overlaps with the signals clustered around 10.1 ppm. The average intensities of signals a and a′ as a function of the added amount of linker are shown in Figure 1B. The signal intensities depend on the equilibria L + A ⇄ LA and LA + A ⇄ ALA, with dissociation constants K_1 and K_2, respectively. Reliable determinations of K_1 and K_2 require concentrations of the reactants at which there is substantial dissociation. Since K_1 and K_2 are expected to be in the micromolar range,[14] and NMR measurements require millimolar quantities for the titrations, no accurate K values could be extracted from Figure 1B. What the data do demonstrate is that the equivalence point in the titration is reached at an [L]/[A] ratio of about 1:2, confirming that one linker molecule associates with two Azu molecules. (The accuracy of the data points in Figure 1B is limited by an uncertainty in the linker concentration and the inherent inaccuracy of the peak intensities caused by line-width variations in the NMR spectra. This explains why the equivalence points are not reached at exactly [L]/[A] = 1:2.)

Crystal Structure of (Zn-H117G)$_2$-1,6-dih Azurin

From diffraction data collected at 100 K, the crystal structure of (Zn-H117G)$_2$-1,6-dih Azu was solved to 2.85 Å resolution (Table 3). Data collected at room temperature showed that the resolution is directly limited by the quality of the crystals and is not affected by the freezing process. The asymmetric unit contains a total of four protein molecules arranged as a pair of dimers (Figure 2), reminiscent of the molecular arrangement observed in crystals of *wt* Azurin.[16] Each of the molecules within the dimer is aligned with its long axis roughly parallel to the 1,6-dih linker. The intramolecular Zn-to-Zn distance amounts to 16.1 Å. The four molecules within the asymmetric unit are superimposable with an RMSD of 0.4 Å for the Cα trace of the entire protein backbone, which diminishes to 0.2 Å when the loop region between residues 116 and 120 is excluded, indicating a well conserved core structure. The Cα trace of Zn-H117G Azu, averaged over all four molecules in the asymmetric unit, is superimposable with *wt* Zn-Azu within 1.1 Å which diminishes to 0.5 Å when residues 116–120 are ignored. The structural details of the metal site are reported in Table 1.

Table 1. Bond lengths and angles between ligands and the metal centre (M) in structures of Azu (*P. aeruginosa*).[a]

Bond lengths [Å]	Cu^{I}-*wt* (1E5Y, 2.0 Å)	Cu^{II}-*wt* (4AZU, 1.9 Å)	Zn^{II}-*wt* (1E67, 2.14 Å)	Zn-H117G-1,6-dih (2.85 Å)
Gly45–M	3.02 (0.06)	2.76 (0.49)	2.32 (0.07)	1.99 (0.01)
His46–M	2.14 (0.07)	2.29 (0.29)	2.07 (0.04)	2.06 (0.02)
Cys112–M	2.29 (0.01)	2.24 (0.04)	2.30 (0.02)	2.34 (0.01)
Met121–M	3.25 (0.06)	3.15 (0.05)	3.38 (0.07)	3.51 (0.15)
His117/Linker–M	2.10 (0.07)	2.01 (0.05)	2.01 (0.03)	2.07 (0.01)
Bond angles [°]				
Sγ112–M–Nδ46	133 (2)	132 (3)	128 (3)	136 (1)
Sγ112–M–Nδ117/Linker	122 (1)	122 (2)	121 (1)	98 (13)
Sγ112–M–Sδ121	113 (1)	110 (1)	103 (1)	99 (2)
Nδ46–M–Sδ121	72 (1)	77 (3)	70 (2)	67 (2)
Nδ46–M–Nδ117/Linker	105 (2)	105 (2)	110 (3)	118 (10)
Sδ121–M–Nδ117/Linker	91 (4)	87 (2)	83 (1)	81 (2)
O45–M–Nδ46	75 (1)	74 (3)	84 (1)	89 (4)
O45–M–Sδ121	145 (1)	148 (2)	152 (2)	152 (3)
O45–M–Nδ117/Linker	87 (2)	89 (1)	98 (2)	102 (4)
O45–M–Sγ112	99 (1)	105 (10)	101 (1)	107 (1)
N_2S–M distance [Å]	0.09 (0.01)	0.06 (0.07)	– 0.16 (0.04)	– 0.32 (0.08)

[a] The bond lengths and angles were obtained by averaging over all the molecules within the asymmetric unit. Numbers between brackets indicate standard deviations.

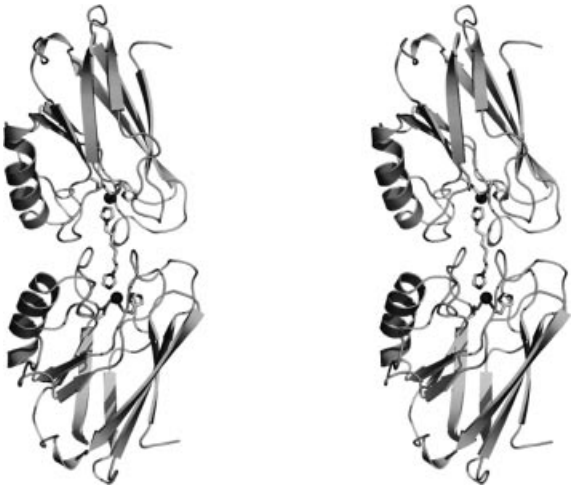

Figure 2. Stereo view of the $(Zn\text{-}H117G)_2$-1,6-dih Azu dimer. The side chains of residues G45, H46, C112, and M121 as well as the 1,6-dih linker are shown as sticks while both zinc atoms are depicted as spheres.

Discussion

Metal Site Structure

Although the limited resolution of the structure of the H117G dimer reported here requires caution with the interpretation of the data, averaging over all of the molecules within the asymmetric unit permits us to compare the structural characteristics of the metal site with those in *wt* Cu^{II}- and Zn^{II}-Azu (Table 1). The main structural difference between the Cu^{II} and Zn^{II} sites in *wt* Azu relates to the decrease in the distance between the metal and the carbonyl of Gly45 and the concomitant increase in the metal–Sδ(Met121) distance when Cu is substituted by Zn. Clearly, the "hard" Zn ion is pulled over from the "soft" sulfur ligand to the "harder" oxygen ligand so that the Zn ion ends up at the other side of the N_2S plane as compared with the Cu ion. A similar observation applies for *wt* Zn-H117G Azurin.[15] The extent to which the structural details of the Zn site in the dimer seem to reproduce those of the *wt* Zn-Azu is remarkable, despite the fact that the imidazole ring is not covalently attached to the protein framework in the dimer. In particular, the positions of the three hard ligands His46, Ser112, and His117/Linker which together form a near-equatorial plane are well conserved. The two axial ligands Met121 and Gly45 show slightly larger deviations relative to *wt* Zn-Azu. They form weak coordinate bonds to the Zn ion and have more positional freedom.

NMR Titration

The NMR titration data (Figure 1) clearly demonstrate that the Zn^{II}-H117G Azu does bind the bifunctional linkers used for this study. The signals used to follow the titration have not been assigned. In native *wt* Cu^{I} Azu there are seven distinct high-field signals in the range of from 9.60 to 11.30 ppm.[27] They derive from the backbone amide protons of Asn38, Asn47, Thr52, Ile87, Thr113, Phe114 and Ser118. Three of these stand out because they occur at very high chemical shift positions: 11.30 (N38), 10.58 (N47) and 10.48 (F114) ppm. Those of N47 and F114, in the *wt* structure, form a H-bridge with the Sγ of the Cys112 metal ligand; their chemical shifts to some extent reflect the charge distribution over the metal site. The amide proton of Asn38 forms a H-bridge with the carboxyl group of Asp11 which is located in the interface of the Zn^{II}-H117G Azu-dimer. One expects these three signals to stand out in the spectrum of the dimer as well, but a definitive identification of the high-field signals a–c and a′–c′ must await a detailed assignment of the spectrum. The low-intensity resonances at 10.14 and 9.96 ppm derive from an apo-Azu impurity.

Ligand Loop Dynamics

Although the overall protein structure of each of the subunits is very similar to *wt* Zn-Azu, the loop on which residues 116 to 119 are located has adopted different conformations in each of the four subunits in the asymmetric unit (Figure 3A). They all have relatively high B factors indicative of increased flexibility (Figure 3B) This flexibility is understandable, given that in H117G Azu the loop is comprised of a series of small, flexible amino acids (Gly-Gly-Ser-Ala) and is consistent with the finding by Jeuken et al. that for Cu^{I}-H117G Azu the residues 116–120 display increased backbone dynamics in solution relative to *wt* Azu.[13]

It is interesting to note that the complete ligand loop runs from Cys112 to Met121 but that only the part running from residues 116–119 shows enhanced disorder. Apparently residues 112–115 are sufficiently strongly anchored to the protein framework to keep them fixed in the structure even when His117 is replaced by a Gly. Of the residues 116–119 in the *wt* structure, only the side chain of His117 is anchored to the protein structure, namely through a bond of the imidazole ring to the Cu. Yet, this is not what keeps His117 in place because in apo-Azu this loop retains its native conformation.[17] It is found that some of the ligand loop residues of Zn^{II}-H117G Azu occur in the disallowed regions of the Ramachandran plot (Figure 4). These dihedral angles have become accessible to the protein only because the His117 has been replaced by a Gly. It is therefore impossible for the ligand loop in *wt* Azu to adopt a configuration as seen here. To what extent the flexibility of the ligand loop in Azu differs from those in other blue copper proteins like plastocyanin, pseudoazurin and amicyanin remains to be seen.

Interface Packing and Solvation

It is of interest to compare the relative orientation of the Azu monomers in the $(Zn\text{-}H117G)_2$-1,6-dih Azu structure with what has been observed for *wt* Azu. For *wt* Azu, the α-helices of the two monomers are situated on opposite sides of the dimer (Figure 5). Covalent dimers of Azu, in

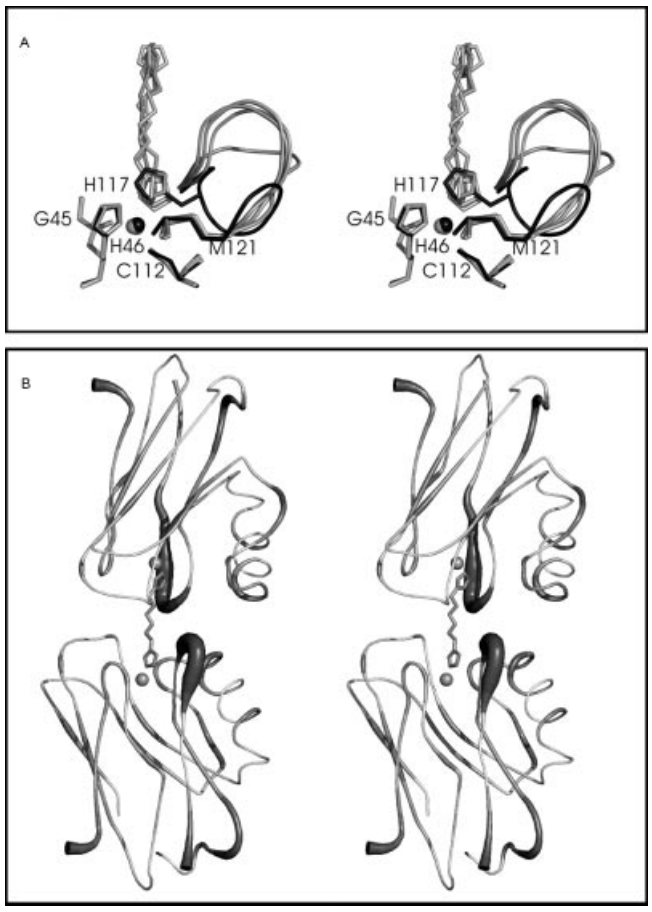

Figure 3. Representation of structural data. (A) Stereo view of residues G45, H46, C112, H/G117 and M121 of each of the monomeric subunits of (Zn-H117G)$_2$-1,6-dih Azu (grey) in the asymmetric unit, superimposed on the structure of Zn-*wt* Azu (black). The ligand loops between residues 115–121 are shown in cartoon representation; the zinc atoms are shown as spheres. Labels correspond to the ligands of *wt* Azu. (B) Stereo image of one of the dimers of (Zn-H117G)$_2$-1,6-dih Azu observed in the asymmetric unit. Darker shading and larger tube diameter indicate increased B factors. The 1,6-dih linker is shown in stick representation; the zinc atoms are shown as spheres. The dimer shown has the most flexible ligand loops of the two dimers found within the asymmetric unit.

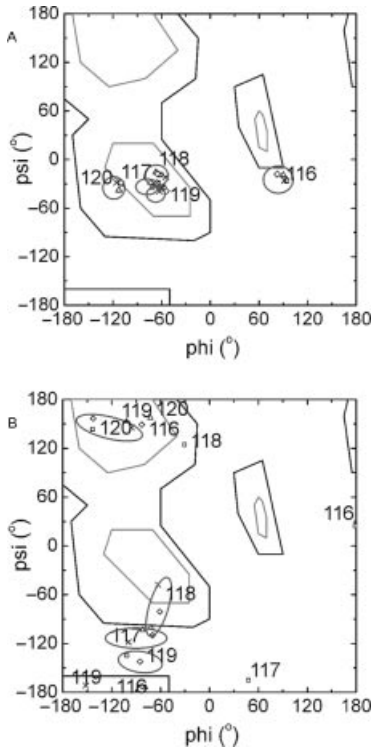

Figure 4. Ramachandran plots of the loop residues 116-120 of (A) Zn-*wt* Azu and (B) (Zn-H117G)$_2$-1,6-dih Azu. Different symbols are used to represent the individual amino acid chains within the asymmetric unit.

Figure 5. Cartoon representations of (Zn-H117G)$_2$-1,6-dih Azu (left) and the crystal packing of Zn-*wt* Azu (right); the α-helical regions are shown in dark grey. The zinc atoms are shown as large spheres (black). Hydrogen-bonded water molecules in the protein interface of *wt* Azu are shown as small spheres (light grey).

which the Azu moieties are connected through a bis(maleimidomethyl) ether (BMME) linker also have a tendency to adopt this orientation.[18] In contrast, the structure of the noncovalent dimer of (Zn-H117G)$_2$-1,6-dih Azu, in which the metal ions are connected with the linker through coordinate Zn-imidazole bonds, has both α-helices on the same side (Figure 5). Somewhat similar orientations have been observed for the C112D and F114A mutants of Azu (1AG0 and 1AZN, respectively).[19,20]

Although the interface area in the dimer is largely retained, its solvent accessibility is slightly larger than that in the structures of *wt* Azu or the BMME-linked N42C Azu-dimer, both of which display the classical hydrophobic interaction packing (Table 2).[16,18,21] A disulfide-linked N42C Azu dimer does not fit in this comparison and is a separate case: its *intra*-dimer interface is very small (ca. 360 Å^2) since two monomers are rotated around the C42–C42 disulfide bond as compared with the *wt* packing. The *inter*-dimer interface is sizeable but smaller than in the *wt* case. The decrease in interface for the (Zn-H117G)$_2$-1,6-dih Azu, however, although not large, is significant and is related to

Table 2. Solvent accessibility and interface area in azurin dimers.

	Accessible surface area [Å^2] per monomer Free[a]	Complex[b]	Interface area [Å^2]
wt (1E5Y) *inter*	6579	6066	1026
N42C-BMME (1JVL) *intra*	6547	6050	995
N42C-disulfide bridged (1JVO) *intra*	6524	6343	363
N42C-disulfide bridged (1JVO) *inter*[c]	6524	6033	983
(Zn-H117G)$_2$-1,6-dih *intra*	6687	6205	964

[a] The coordinate file used for the calculation contained a single monomer; additional monomers were removed from the asymmetric unit. [b] The coordinate files used for the calculation were edited to contain only the molecules that share the contact surface under consideration. [c] Numbers correspond to the intermolecular interface between two different dimers in the asymmetric unit.

the packing of the monomers. From previous experiments on H117G Azu it was concluded that 1,5-dip gives optimal packing of the Azu monomers and that 1,6-dih Azu is slightly too long to let monomers approach as close as in the *wt* case.[14] The increase in metal-to-metal distance in the Zn-H117G Azu dimer (16.1 Å *vs.* 14.9 Å in *wt* Azu[16]) is in line with this conclusion. A slightly larger distance between the two Azu halves in the dimer would also mean a smaller contact area, in agreement with the data in Table 2.

The findings reported here and in the preceding discussion show that the packing of two Azu molecules with their hydrophobic patches together is thermodynamically favourable. Previous experiments have shown that the gain in free energy when two Azu molecules associate is 2.1 kcal/mol.[14] The present data show that Azu molecules prefer to pack with their hydrophobic patches opposite to each other, but that the precise mutual orientation of the monomers may vary and probably depends on small variations in the free energy of association caused by small adjustments in the van der Waals energy, remote charge effects and the precise configuration of hydrogen bridges across the interface.

Conclusions

Site-directed mutagenesis of the copper ligand H117 of the blue copper protein Azu (*P. aeruginosa*) creates a solvent-exposed aperture in the protein, which can accommodate a variety of ligands, thereby permitting "hotwiring" of the protein. Incubation of the H117G variant with bifunctional linkers like the 1,ω-di(imidazol-1-yl)-*n*-alkanes allows the formation of Azu dimers noncovalently linked by the functionalized alkanes. The (Zn-H117G)$_2$-1,6-dih Azu dimer was crystallized and its structure was solved to 2.85 Å resolution. Relative to *wt* Azu, H117G Azu shows increased flexibility in the loop region between residues 116–120, surrounding the site of mutation. The displacement of this loop from the protein interior may facilitate the coordination of larger exogenous ligands. The structure represents a type of dimer in which the proteins have adopted a relative orientation distinct from those previously reported for dimers of Azu.

Experimental Section

Protein Expression and Isolation: Apo-H117G Azu was produced and purified as described previously. The concentration of apoprotein was determined from the absorbance at 280 nm (ε_{280} = 9.1 ± 0.1 mM^{-1} cm^{-1}) recorded at room temperature (r.t.) on a Perkin–Elmer lambda 18 spectrophotometer.

Linkers: The bifunctional ligands (Figure 1A) 1,5-di(imidazol-1-yl)pentane and 1,6-di(imidazol-1-yl)hexane were synthesized as previously reported.[14] Purity and integrity of the samples after prolonged storage was confirmed by ^{1}H NMR and working solutions of 6 mM were prepared in MilliQ grade water.

NMR Spectroscopy: All ^{1}H NMR spectra were recorded with a Bruker Avance DMX 600 MHz spectrometer at 304 K with a spectral width of 12.98 ppm in 4 K memory by using a Watergate-filtered pulse sequence. Free induction decays were Fourier transformed by using a squared sine window function. All samples were prepared in potassium phosphate (KP_i), pH 6.5 buffer (20 mM) supplemented with 6% D_2O for locking of the signal. The binding of 1,6-dih to Zn-H117G Azu was assessed by addition of linker (0.7 equiv.) to a solution of apo-H117G Azu (0.5 mM). After recording of the ^{1}H NMR spectrum, $Zn(SO_4)_2$ (2 equiv.) was added, and the sample was incubated at r.t. for ca. 10 min allowing coordination of the linker to the reconstituted protein. The effects of coordination of 1,6-dih or 1,5-dip on the ^{1}H NMR spectra of Zn-H117G Azu were compared by titration of protein (1 mM) in KP_i, (20 mM, pH 6.5) with either of the linkers. Zn-H117G Azu was prepared by incubating a solution of the apoprotein at the desired concentration with $ZnSO_4$ (1.2 equiv.) for 10 min at r.t. This solution was used as prepared.

Crystallization and X-ray Data Collection: A solution of apo-H117G Azu (10 mg/mL) in Tris-HCl (10 mM, pH 7.5) was incubated with $ZnCl_2$ (1.3 equiv.) for 2 h at r.t. Excess $ZnCl_2$ was removed by ultracentrifugation (Centricon, MWCO 10,000). The sample was then incubated with either 1,5-dip (0.6 equiv.) or 1,6-dih (0.6 equiv.). Prior to crystallization the samples were filtered through a low-protein-binding, 0.22-μm filter (Millipore). Crystals of (Zn-H117G)$_2$-1,6-dih were obtained by sitting drop vapour diffusion at 295 K by using equal volumes of protein and reservoir solution. Crystals suitable for X-ray crystallography appeared within 3 d, from protein solution (1 μL) mixed with reservoir solution (1 μL) containing Tris-HCl (100 mM, pH 8.56) and 20% (w/v) polyethylene glycol (PEG) 8000. No crystals were obtained for (Zn-H117G)$_2$-1,5-dip. X-ray diffraction data of (Zn-H117G)$_2$-1,6-dih were collected on an in-house beam by using a MAR345 Image Plate detector. A crystal was mounted in a cryo-loop (Hampton Research) and passed quickly through a cryo-protectant solution

containing 20% glycerol, followed by flash-freezing in a nitrogen gas stream at 100 K. A data set was collected to 2.85 Å resolution. All collected data were indexed, integrated and scaled with HKL2000.[22] Data collection and refinement statistics can be found in Table 3.

Table 3. X-ray diffraction data collection, refinement and model statistics.

Data collection	
Space group	*P*1
Unit cell parameters $a \times b \times c$ [Å]	42.66 × 49.72 × 66.07
Resolution [Å][a]	25–2.85 (2.9–2.85)
Measured reflections	28364
Unique reflections	11979
Completeness (%)	88.2
R_{merge}[b] (%)	8.7 (34.1)
Average *I*/sigma (*I*)	9.36 (1.83)
Refinement statistics	
R-factor (%)	19.2 (32.5)
Free *R*-factor (%)	23.3 (44.7)
Average total B-value protein [Å^2]	30.5
Model statistics	
Number of TLS groups	4
Number of monomers in the asymmetric unit	4
Number of protein residues	512
Number of solvent molecules	3
Number of Zn ions	4
Number of ligands	2
Ramachandran plot (%)	
Most favoured region	89.5
Additionally favoured region	10.2
Generally favoured region	0.2
Disallowed region	0.1
R.m.s. deviation from ideality	
Bond lengths [Å]	0.013
Bond angles [°]	1.070

[a] Values of reflections recorded in the highest resolution shell are shown in parentheses. [b] $R_{merge} = \Sigma_o(|I-<I>|)/\Sigma(I)$ (scalepack output). The coordinates have been deposited in the Protein Data Bank under accession code 2IWE.

Structure Determination and Refinement: The structure of (Zn-H117G)$_2$-1,6-dih was solved by molecular replacement by using the program Molrep[23] from the CCP4 program suite[24] by employing the structure of Zn-*wt* Azu (PDB entry 1E67)[15] as a search model. A solution was obtained with an *R* factor of 39.7% and a correlation coefficient of 58.8. After several rounds of rigid-body and restrained refinement with Refmac5,[25] the mutated amino acids were built in manually with Xtalview,[26] followed by automatic solvent building with ARP/wARP.[27] Upon inspection of an $F_o - F_c$ difference density map, a double conformation of the main chain running from residue G116 to M121 of molecule A could be modelled and refined, leading to an improvement of R_{free}. Extra density was also observed for this flexible loop in the three other molecules present in the asymmetric unit but was considered too weak to build any amino acids. Final refinement by using tight NCS restraints between residues 1 to 114 of each protein chain and refinement of translation, liberation and screw (TLS) parameters[28] resulted in a model with an *R* factor of 19.2% (R_{free} 23.3%). The quality of the model was checked by PROCHECK[29] and WHATIF[30] (see Table 3). The coordinates and structure factors have been deposited in the Protein Data Bank under accession code 2IWE. Figure 2, Figure 3 and Figure 5 were made in PyMOL 0.98.[31] Figure 3 was generated with the help of the color_b.py script for colouring according to B factor (http://adelie.biochem.queensu.ca/~rlc/).

Solvent Accessibility and Interface Areas: The solvent-accessible surface area (ASA) was calculated by using the program NACCESS 2.1.1 with a probe radius of 1.4 Å. The interface area was defined as the sum of the ASAs of the individual proteins minus the ASA of the complex.

[1] I. Hamachi, S. Shinkai, *Eur. J. Org. Chem.* **1999**, 539–549.
[2] T. Hayashi, Y. Hitomi, T. Takimura, A. Tomokuni, T. Mizutani, Y. Hisaeda, H. Ogoshi, *Coord. Chem. Rev.* **1999**, *192*, 961–974.
[3] A. Riklin, E. Katz, I. Willner, A. Stocker, A. F. Buckmann, *Nature* **1995**, *376*, 672–675.
[4] T. den Blaauwen, M. van de Kamp, G. W. Canters, *J. Am. Chem. Soc.* **1991**, *113*, 5050–5052.
[5] H. J. Wijma, M. J. Boulanger, A. Molon, M. Fittipaldi, M. Huber, M. E. P. Murphy, M. P. Verbeet, G. W. Canters, *Biochemistry* **2003**, *42*, 4075–4083.
[6] H. Nar, A. Messerschmidt, R. Huber, M. van de Kamp, G. W. Canters, *J. Mol. Biol.* **1991**, *218*, 427–447.
[7] E. Vijgenboom, J. E. Busch, G. W. Canters, *Microbiology* **1997**, *143*, 2853–2863.
[8] M. van de Kamp, M. C. Silvestrini, M. Brunori, J. van Beeumen, F. C. Hali, G. W. Canters, *Eur. J. Biochem.* **1990**, *194*, 109–118.
[9] M. van de Kamp, R. Floris, F. C. Hali, G. W. Canters, *J. Am. Chem. Soc.* **1990**, *112*, 907–908.
[10] T. den Blaauwen, G. W. Canters, *J. Am. Chem. Soc.* **1993**, *115*, 1121–1129.
[11] T. den Blaauwen, C. W. G. Hoitink, G. W. Canters, J. Han, T. M. Loehr, J. Sanders-Loehr, *Biochemistry* **1993**, *32*, 12455–12464.
[12] C. Hammann, G. van Pouderoyen, H. Nar, F. X. G. Ruth, A. Messerschmidt, R. Huber, T. den Blaauwen, G. W. Canters, *J. Mol. Biol.* **1997**, *266*, 357–366.
[13] L. J. C. Jeuken, M. Ubbink, J. H. Bitter, P. van Vliet, W. Meyer-Klaucke, G. W. Canters, *J. Mol. Biol.* **2000**, *299*, 737–755.
[14] G. van Pouderoyen, T. den Blaauwen, J. Reedijk, G. W. Canters, *Biochemistry* **1996**, *35*, 13205–13211.
[15] H. Nar, R. Huber, A. Messerschmidt, A. C. Filippou, M. Barth, M. Jaquinod, M. van de Kamp, G. W. Canters, *Eur. J. Biochem.* **1992**, *205*, 1123–1129.
[16] H. Nar, A. Messerschmidt, R. Huber, M. van de Kamp, G. W. Canters, *J. Mol. Biol.* **1991**, *221*, 765–772.
[17] H. Nar, A. Messerschmidt, R. Huber, M. van de Kamp, G. W. Canters, *Febs Lett.* **1992**, *306*, 119–124.
[18] I. M. C. van Amsterdam, M. Ubbink, O. Einsle, A. Messerschmidt, A. Merli, D. Cavazzini, G. L. Rossi, G. W. Canters, *Nat. Struct. Biol.* **2002**, *9*, 48–52.
[19] S. Faham, T. J. Mizoguchi, E. T. Adman, H. B. Gray, J. H. Richards, D. C. Rees, *J. Biol. Inorg. Chem.* **1997**, *2*, 464–469.
[20] L. C. Tsai, L. Sjolin, V. Langer, T. Pascher, H. Nar, *Acta Crystallogr., Sect. D* **1995**, *51*, 168–176.
[21] I. M. C. van Amsterdam, M. Ubbink, L. J. C. Jeuken, M. P. Verbeet, O. Einsle, A. Messerschmidt, G. W. Canters, *Chem. Eur. J.* **2001**, *7*, 2398–2406.
[22] Z. Otwinowski, W. Minor, *Methods Enzymol.* **1997**, *276*, 307–326.
[23] A. Vagin, A. Teplyakov, *J. Appl. Crystallogr.* **1997**, *30*, 1022–1025.
[24] S. Bailey, *Acta Crystallogr., Sect. D* **1994**, *50*, 760–763.
[25] G. N. Murshudov, A. A. Vagin, E. J. Dodson, *Acta Crystallogr., Sect. D* **1997**, *53*, 240–255.
[26] D. E. McRee, *J. Struct. Biol.* **1999**, *125*, 156–165.

[27] V. S. Lamzin, K. S. Wilson, *Acta Crystallogr., Sect. D* **1993**, *49*, 129–147.
[28] M. D. Winn, M. N. Isupov, G. N. Murshudov, *Acta Crystallogr., Sect. D* **2001**, *57*, 122–133.
[29] R. A. Laskowski, M. W. MacArthur, D. S. Moss, J. M. Thornton, *J. Appl. Crystallogr.* **1993**, *26*, 283–291.
[30] G. Vriend, *J. Mol. Graph.* **1990**, *8*, 52–56.
[31] W. L. DeLano, *The PyMOL Molecular Graphics System* (http://www.pymol.org), San Carlos, CA, USA **2002**.

Received: June 19, 2006
Published Online: September 5, 2006

